Research Article

Journal of Environmental Nanotechnology

Application of the Taguchi Method to Optimize the Process Parameters of a Single-slope Solar Still Integrated with a Solar Pond

M. Koilraj[1], K. Suresh[2], Eastus Russel[3], M. Yuvaperiyasamy[4*], R. Paullinga Prakash[5] and M. Karthigairajan[6]

[1]Department of Mechanical Engineering, Oxford Engineering College, Tiruchirappalli, TN, India
[2]Department of Electrical & Electronics Engineering, Karpaga Vinayaga College of Engineering and Technology, Chengalpattu, TN, India
[3]Department of Mechanical Engineering, Sri Muthukumaran Institute of Technology, Chikkarayapuram, Chennai, TN, India
[4]Department of Mechanical Engineering, Saveetha Institute of Medical and Technical Sciences, Chennai, TN, India
[5]Department of Mechanical Engineering, Vel Tech Multitech Dr. Rangarajan Dr. Sakunthala Engineering College, Chennai, TN, India
[6]Department of Mechanical Engineering, Karpaga Vinayaga College of Engineering and Technology, Chengalpattu, TN, India
Received: 07.07.2025 Accepted: 04.09.2025 Published: 30.09.2025
*yuvaperiyasamyvsb@gmail.com

ABSTRACT

This study employs the Taguchi optimization method to enhance the performance of a single-slope solar still (SSSS) integrated with a solar pond. Key variables, including solar radiation (600 to 1000 W/m²), water depth (4 to 8 cm), inlet water temperature (30 to 40 °C), and wind speed (1 to 5 m/s), were tested using an L_9 orthogonal array. Signal-to-noise ratio analysis was used to identify optimal settings, while analysis of variance determined the most significant factors. Regression analysis established the relationship between input parameters and system outputs, including freshwater yield and basin water temperature. The highest productivity was achieved under conditions of 1000 W/m² solar radiation, a 4 cm water depth, a 3 m/s wind velocity, and a 40 °C inlet temperature. Under optimized conditions, the solar still exhibited a predicted productivity of 1.131 kg/m², with an experimental deviation of 9.31%. The basin water temperature showed a minimal deviation of 2.18%. These results technically confirm the robustness of the regression models and the reliability of the optimized process parameters. The strong agreement between predicted and observed values confirms the reliability of the model and the effectiveness of the optimization strategy in improving the solar still performance.

Keywords: Taguchi method; Solar still; Solar pond; ANOVA; Regression analysis; Freshwater productivity; Process optimization; Water temperature.

1. INTRODUCTION

Access to clean, safe freshwater is essential for sustaining human health, enhancing agricultural productivity, and fostering industrial development. Freshwater shortages represent a significant global issue, particularly in arid and semi-arid regions where natural water resources are constrained. The significant rise in population, urban development, and climate change intensifies the demand on existing water resources, highlighting the need for the creation of sustainable and economically viable water purification systems (Ashok and Sakthivel, 2025). Solar desalination offers a viable solution to address freshwater limitations by harnessing abundant and renewable solar energy to convert saltwater or brackish water into potable water. Among various solar desalination methods, the solar still (SS) represents a simple, cost-effective, and environmentally sustainable technology that mimics the natural hydrological cycle. However, its practical application is often limited by relatively low productivity. To improve efficiency, various design modifications and optimization techniques have been explored (Jha and Ghosh, 2025). Recent studies have shown that modifying SSs with black-coated corrugated absorbers and zeolite crystals can increase the daily yield from 3–5 L/m² to 8–13 L/m². Integrating evacuated tube collectors can further boost productivity by up to 175%. Pyramid SSs, especially with hybrid enhancements, are the most efficient for arid and remote regions (Hussein *et al.* 2024). Studies show that active SSs with parabolic trough collectors achieve the highest productivity at 12.4 L/m²/day, while double-slope stills improve output by 50% over passive types. Hybrid SSs exhibited the lowest water cost at $0.009/L, demonstrating strong economic viability (Almajali *et al.* 2025).

A novel solar still utilizing black-coated cylindrical cement fins encased in black cotton fabric achieved a maximum freshwater output of 4,440 mL/m²/day, indicating a 64.3% improvement over conventional designs. It achieved the best energy and exergy efficiencies (42.4% and 3.7%), along with the lowest cost per liter at $0.010/L, underscoring its

performance and sustainability advantages (Kumar *et al.*, 2025a). SSs with cylindrical cement fins (SSCCF) demonstrated a 27% increase in yield and a 23% reduction in cost compared to CSS at a water depth of 2 cm, achieving a maximum production of 4462.4 mL/m²/day and an efficiency of 41.5%. With a 26% improvement over the standard design, carbon credits were able to mitigate carbon emissions 110.87% more effectively (Kumar *et al.* 2025b). A portable double-slope solar still, employing PMMA (polymethyl methacrylate) covers and integrated thermal management components (insulation, aluminum, and phase change materials), produced a daily freshwater yield of 385 mL and demonstrated a performance improvement of up to 45.2%. The total dissolved solids (TDS) decreased by 95.8%, lowering concentrations from 4970 ppm to below 200 ppm, thus meeting the World Health Organization's drinking water standards (Kouravand *et al.* 2025). In studies conducted in Bhopal, an SS using ZnO nanofluids attained a maximum temperature of 69.8 °C and an efficiency of 29.50%, surpassing the non-nanofluid still, which reached 63.8 °C and an efficiency of 20.14%. Efficiency gains using SiO_2, ZnO, and their blend were 22.53%, 29.50%, and 25.24%, respectively, demonstrating significant improvements in thermal performance (Sahu and Tiwari, 2024).

Integrating solar collectors with traditional SSs increased productivity to 4.766 L/m²/day using finned tube and 3.853 L/m²/day using flat plate collectors, representing 65.12% and 33.49% improvements over the conventional solar stills (CSSs) at 2.886 L/m²/day. A cost study indicated that the finned tube solar collector system had the lowest cost per liter (Abdulridha *et al.* 2024). Experiments conducted in Tunisia demonstrated that the application of 1.8 kg of phase change materials (PCMs) with internal reflectors resulted in a 124.74% increase in SS production during spring and a 51.91% increase in summer when using soy wax. This performance exceeded that of Vaseline, which achieved increases of 110.68% in spring and 45.72% in summer, as well as paraffin wax, which recorded increases of 103.18% in spring and 43.35% in summer. The lowest cost per liter was achieved with soy wax at $0.041, compared to $0.045 for conventional soy wax (Saad *et al.*, 2024). A comparative analysis indicated that spherical solar stills achieved a maximum output of 5.5 kg/m²/day and an efficiency of 44%, surpassing hemispherical designs, which produced 4.45 kg/m²/day with an efficiency of 40.5%, as well as single-slope configurations (3.1 kg/m²/day, 35%). Productivity rose by 77.42% for spherical stills and 43.55% for hemispherical stills compared to the single-slope arrangement (Kabeel *et al.* 2024). Modified SSs employing various absorber materials revealed that steel wool pads achieved the highest output of 4.384 L/m²/day and a thermal efficiency of 32.74%. The minimum cost per liter was $0.0034, indicating the superior efficiency and cost-effectiveness of steel wool pads relative to alternative materials (Ramzy *et al.* 2023). The application of 4 kg of RT42 phase change material in a single-slope solar still resulted in a 29.7% increase in freshwater production, achieving an average daily efficiency of 66.7%, compared to 51.5% for a conventional solar. The productivity with 4 kg of PCM exceeded that with 2 kg and 6 kg of PCM by 18.6% and 27.7%, respectively (Mohammed *et al.* 2024). The use of a rock stone bed as an energy storage medium in an SS system resulted in an 18.6% increase in freshwater production compared to a CSS system. The system demonstrated improved energy efficiency and produced water suitable for domestic use, offering a low-cost, locally implementable solution (Karthick *et al.* 2022).

Despite extensive enhancements to SSs using PCMs, nanofluids, and design modifications, the integration of solar ponds as sustainable heat sources with various operational parameters remains underexplored. Moreover, statistical optimization of such hybrid systems is scarcely addressed. This study fills these gaps by integrating a solar pond with an SSSS and applying the Taguchi method to optimize key operating parameters, resulting in improved thermal performance and productivity.

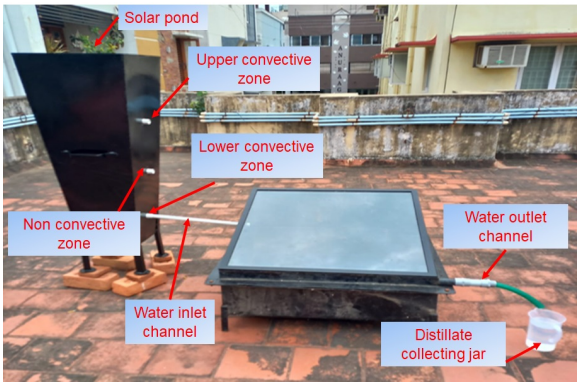


Fig. 1: Single-slope Solar Still with solar pond

2. MATERIALS AND METHODS

2.1 Experimental Setup and Experimental Procedure

A SSSS was constructed utilizing a 5 mm thick galvanized iron sheet to create a basin with an effective area of 1 m². The still's upper section was fitted with a 4 mm thick transparent glass sheet, inclined at 13 degrees, aligning with the latitude of the experimental site in Chennai, to promote efficient dropwise condensation and facilitate the smooth runoff of distilled water. A short plastic inlet pipe was fixed at the front end to supply saline water into the basin, while a similar outlet pipe was installed at the rear end to collect the condensed water through a sloped channel connected beneath the glass cover. To minimize heat losses and improve thermal efficiency, the outer surfaces of the still were insulated

using 5 cm thick thermocol, a material with low thermal conductivity.

Additionally, a miniature solar pond was positioned nearby to enhance the thermal energy input to the still. The pond was constructed from galvanized sheet metal, measuring 45 cm by 45 cm in top dimension, 30 cm by 30 cm in bottom dimension, and 150 cm in height. It was hydraulically connected to the SS through a plastic pipe located at a vertical position of 30 cm, referred to as the lower thermal zone, to facilitate stratified heat transfer from the pond to the still.

This integrated system was tested under real-time conditions at SIMATS Engineering, Chennai (13.0843° N, 80.2705° E), India. The experiments were conducted over six consecutive days, from March 25 - 30, 2025, with daily data collection taking place from 8:00 a.m. to 6:00 p.m. to assess the performance of the SS and the efficacy of the coupled solar pond system.

Table 1 presents the detailed uncertainty analysis associated with the experimental measurements conducted during the performance evaluation of the SS system. The study includes the measurement instruments, operational ranges, least counts, and related uncertainties, ensuring the precision and reproducibility of the acquired data.

Table 1. Instruments used with their error %

Measured parameter	Instrument used	Range	Least count	Accuracy	Uncertainty (±)
Temperature (°C)	K-type Thermocouple	0–1000	0.1	±0.5% of reading	±0.5 °C
Solar Intensity (W/m²)	Pyranometer	0–2000	1	±10 W/m²	±10 W/m²
Water Depth (cm)	Graduated scale	0–10	0.1	±1 mm	±0.1 cm
Distillate Collector (mL)	Graduated Measuring Cylinder	0–1000	1	±0.5% of reading	±5 mL
Wind Velocity (m/s)	Digital Anemometer	0–30	0.1	±2% of reading	±0.2 m/s

2.2 Taguchi Method

Taguchi methods are robust statistical techniques for optimizing process parameters and improving quality by minimizing variation through a reduced number of experiments (Aksoğan and Toptaç, 2025). The method employs orthogonal arrays (OAs) to systematically study the effects of multiple factors with minimal trials. A fundamental statistic in Taguchi analysis is the Signal-to-Noise (S/N) ratio, which measures the stability of performance (Thiyagarajan *et al.* 2025). Table 2 presents the input process parameters and their corresponding levels. Depending on the objective, the S/N ratio is calculated using formulas such as (Fatima *et al.* 2025):

Larger-the-Better

$$\frac{S}{N} = -10\log_{10}\left(\frac{1}{n}\sum_{i=1}^{n}\frac{1}{y_i^2}\right) \quad \ldots (1)$$

Smaller-the-Better

$$\frac{S}{N} = -10\log_{10}\left(\frac{1}{n}\sum_{i=1}^{n}y_i^2\right) \quad \ldots (2)$$

Nominal-the-Best

$$\frac{S}{N} = -10\log_{10}\left(\frac{\bar{y}^2}{s^2}\right) \quad \ldots (3)$$

where,

y_i: individual measured value
n: number of repetitions (trials)
$\bar{y}$: mean of observations
s^2: variance of observations

Table 2. Input process parameters and their levels

S. No.	Parameters	Levels		
		Low	Medium	High
1	Solar radiation (W/m²)	600	800	1000
2	Water depth (cm)	4	6	8
3	Water inlet temperature (°C)	30	35	40
4	Wind velocity (m/s)	1	3	5

2.3 Analysis of Variance (ANOVA)

Analysis of Variance (ANOVA) is employed to quantify the contribution of each input parameter to the output response by partitioning the total variation into factor-specific and error components, thereby identifying statistically significant influences on system performance (Liu and Zhu, 2025). This statistical approach highlights the contribution of each parameter, allowing for the determination of optimal settings that enhance quality while minimizing variability. By focusing on the most

influential factors, ANOVA guides effective process optimization and quality improvement (Antony *et al.* 2024)

Analysis of Variance (ANOVA) was applied to the experimental data obtained from the Taguchi L_9 orthogonal array design to quantify the influence of process parameters such as solar radiation, water depth, wind velocity, and inlet water temperature on the productivity and basin water temperature of the single-slope solar still integrated with a solar pond. Using statistical software, the total variation in the output responses was divided into contributions from each input factor and experimental error.

3. RESULTS AND DISCUSSION

Table 3 summarizes the impact of solar radiation, water depth, inlet temperature, and wind velocity on the SS's productivity and basin water temperature. An increase in solar radiation enhances thermal energy availability, resulting in elevated basin water temperatures and promoting increased evaporation and distillate yield (Yuvaperiyasamy *et al.* 2023). Similarly, higher inlet water temperature reduces the additional thermal energy required to initiate evaporation, resulting in improved system efficiency. In contrast, increased water depth raises the thermal mass of the basin water, delaying its heating and subsequently reducing the evaporation rate (Yuvaperiyasamy *et al.* 2025). Wind velocity influences both condensation and heat loss; at moderate levels, it enhances convective cooling at the glass surface, thereby improving condensation and water collection. Excessive wind velocity enhances convective heat losses from the basin surface, resulting in a decrease in basin water temperature and a reduction in overall productivity (Dhivagar and Mohanraj, 2021). These results highlight the importance of optimizing each parameter for maximum efficiency and distillate yield.

Table 3. Experimental findings using the Taguchi optimization approach

Run	Solar Radiation (W/m^2)	Water Depth (cm)	Wind Velocity (m/s)	Inlet Water Temperature (˚C)	Productivity (kg/m^2)	Water Temperature (˚C)
1	600	4	1	30	0.365	49.20
2	600	6	3	35	0.453	51.15
3	600	8	5	40	0.496	49.88
4	800	4	3	40	1.125	55.30
5	800	6	5	30	0.640	51.25
6	800	8	1	35	0.535	51.15
7	1000	4	5	35	0.855	54.20
8	1000	6	1	40	0.958	52.50
9	1000	8	3	30	0.655	53.20

Table 4 presents the response table for SN ratios related to productivity, where the Delta values quantify the variation in performance across different levels of each factor. Solar radiation exhibits the highest Delta value (5.438), confirming its dominant role in enhancing thermal energy input and evaporation rate. The water inlet temperature (3.622) significantly contributes to reducing the thermal lag in reaching evaporation conditions. Water depth (2.036) influences basin heat retention, with lower depths improving thermal responsiveness. Wind velocity (1.677) shows the least effect, as its impact on condensation is secondary. The order of factor influence on productivity is: solar radiation > water inlet temperature > water depth > wind velocity.

Fig. 2 presents the Main Effects Plot of S/N ratios, illustrating the influence of each input on productivity. The SN ratio increases markedly with solar radiation, reaching its peak at 1000 W/m², indicating enhanced evaporation at higher irradiance levels. Water depth exhibits a negative trend, with the highest productivity observed at a depth of 4 cm, due to reduced thermal inertia. Productivity increases with inlet temperature, peaking at 40 °C, while wind velocity has a minimal impact, showing a slight improvement at 3 m/s. Optimal conditions are 1000 W/m² solar radiation, 4 cm water depth, 3 m/s wind speed, and 40 °C inlet temperature.

Table 4. S/N ratio response for Productivity

Level	Solar Radiation (W/m^2)	Water Depth (cm)	Wind Velocity (m/s)	Inlet Water Temperature (˚C)
1	-7.241	-3.031	-4.853	-5.435
2	-2.762	-3.709	-3.177	-4.557
3	-1.803	-5.066	-3.776	-1.813
Delta	5.438	2.036	1.677	3.622
Rank	1	3	4	2

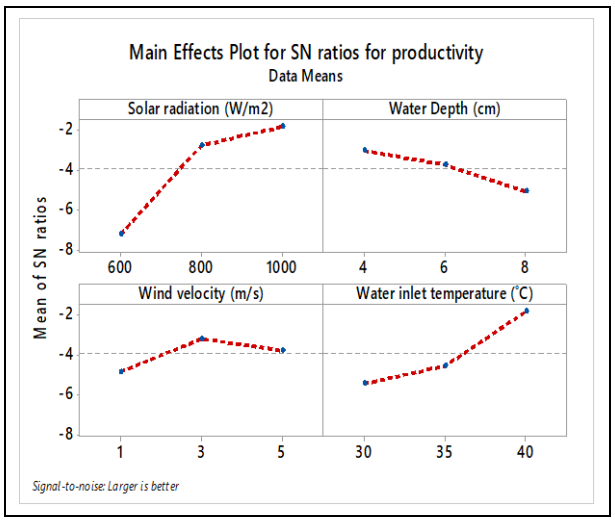


Fig. 2: S/N ratio plot for Productivity

Table 5 presents the S/N ratio response for water temperature, with Delta values indicating the range of each parameter's effect. Solar radiation shows the highest Delta (0.54), suggesting it is the most influential factor, as increased irradiance enhances thermal energy absorption in the basin water. Wind velocity ranks second (Delta = 0.38), likely due to its role in improving convective heat transfer over the water surface. Water depth (Delta = 0.24) ranks third, where lower depths enable quicker heating due to reduced thermal mass. The water inlet temperature has the least influence ($\Delta = 0.22$), as its effect is limited to the initial heating. The order of influence is: solar radiation > wind velocity > water depth > water inlet temperature.

Table 5. S/N ratio response for Water temperature

Level	Solar Radiation (W/m^2)	Water Depth (cm)	Wind Velocity (m/s)	Inlet Water Temperature (°C)
1	33.99	34.46	34.14	34.18
2	34.41	34.26	34.52	34.34
3	34.53	34.22	34.28	34.41
Delta	0.54	0.24	0.38	0.22
Rank	1	3	2	4

Fig. 3 displays the Main Effects Plot of S/N ratios for water temperature, highlighting the influence of each parameter. Solar radiation has the most significant impact, with the SN ratio increasing steadily and peaking at 1000 W/m² due to enhanced thermal input. Water depth exhibits a declining trend, with the highest S/N ratio at 4 cm, as shallower water heats more rapidly. Wind velocity peaks at 3 m/s, indicating improved convective heat transfer at moderate airflow rates. The water inlet temperature has a slight positive effect, with the maximum SN ratio occurring at 40 °C. The optimal conditions for maximum water temperature are 1000 W/m² of solar radiation, a 4 cm water depth, a 3 m/s wind speed, and an inlet temperature of 40 °C.

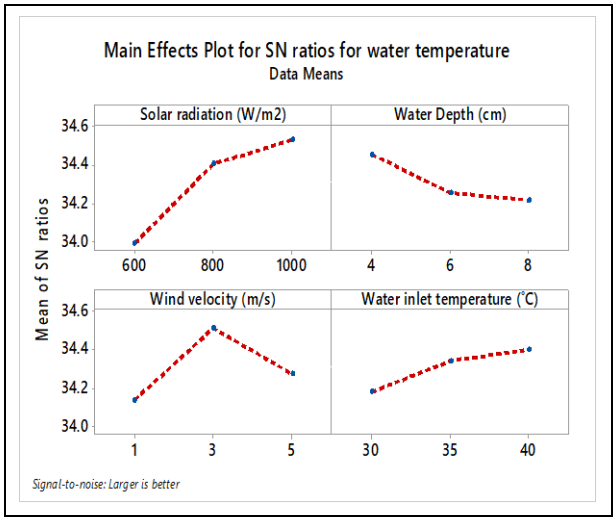


Fig. 3: S/N ratio plot for Water temperature

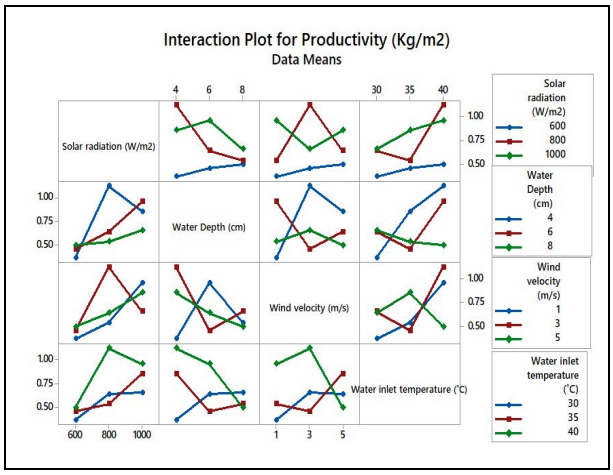


Fig. 4: Interaction effects of input parameters on Productivity

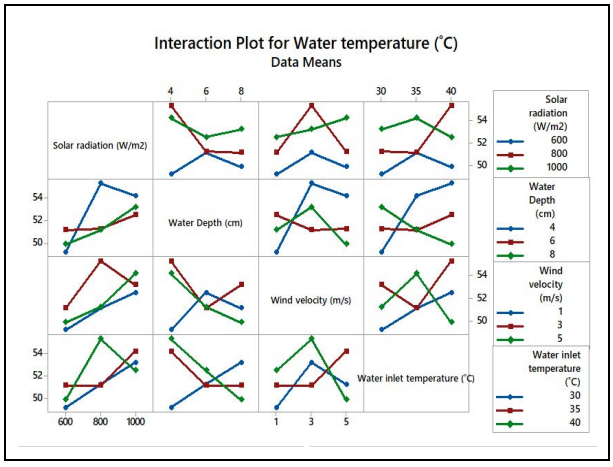


Fig. 5: Interaction effects of input parameters on Water temperature

Fig. 4 illustrates the interaction plot for productivity, showing the combined effects of the process parameters. Significant interactions are observed, particularly between solar radiation and water depth, where maximum productivity occurs at 1000 W/m² and a depth of 4 cm. Similarly, solar radiation and water inlet temperature exhibit a strong interaction, with peak output at 40 °C. Wind velocity influences both water depth and inlet temperature, with a velocity of 3 m/s producing optimal results under ideal conditions. The presence of intersecting, non-parallel lines confirms that parameter effects are interdependent, emphasizing the importance of combined optimization.

Fig. 5 displays the interaction plot for water temperature, illustrating the combined influence of input parameters on thermal performance. Significant interactions occur between solar radiation and water depth, with maximum temperatures reached at 1000 W/m² and a depth of 4 cm. The interaction between water inlet temperature, wind velocity, and solar radiation is notable, with peak values observed at an inlet temperature of 40 °C and a wind velocity of 3 m/s. The intersecting, non-parallel lines confirm that water temperature depends on the interdependent effects of parameters, highlighting the necessity of integrated optimization for enhanced system efficiency.

Table 6. Basic ANOVA for Productivity

Source	DF	Adj SS	Adj MS	F-value	P-value
Solar radiation (W/m^2)	2	0.25913	0.12956	*	*
Water depth (cm)	2	0.07266	0.03633	*	*
Wind velocity (m/s)	2	0.02410	0.01205	*	*
Water inlet temperature (˚C)	2	0.15775	0.07887	*	*
Error	0	*	*		
Total	8	0.51363			

Table 7. Basic ANOVA for Water Temperature

Source	DF	Adj SS	Adj MS	F-value	P-value
Solar radiation (W/m^2)	2	17.128	8.564	*	*
Water depth (cm)	2	3.874	1.937	*	*
Wind velocity (m/s)	2	7.895	3.947	*	*
Inlet water temperature (˚C)	2	2.862	1.431	*	*
Error	0	*	*		
Total	8	31.759			

Table 8. Pooled ANOVA results for Productivity

Source	DF	Adj SS	Adj MS	F-value	P-value	% Contribution
Solar radiation (W/m^2)	2	0.25913	0.12956	10.75	0.085	50.45
Water depth (cm)	2	0.07266	0.03633	3.02	0.249	14.15
Inlet water temperature (˚C)	2	0.15775	0.07887	6.55	0.133	30.71
Error	2	0.02410	0.01205			4.69
Total	8	0.51363				100

Table 9. Pooled ANOVA results for Water Temperature

Source	DF	Adj SS	Adj MS	F-value	P-value	% Contribution
Solar radiation (W/m^2)	2	17.128	8.564	5.99	0.143	53.93
Water depth (cm)	2	3.874	1.937	1.35	0.425	12.20
Wind velocity (m/s)	2	7.895	3.947	2.76	0.266	24.86
Error	2	2.862	1.431			9.01
Total	8	31.759				100

ANOVA identifies the key process parameters that influence performance. Tables 6 and 7 present the initial ANOVA results for productivity and water temperature. However, due to zero degrees of freedom, F and P values could not be computed. To address this, ANOVA pooling was performed by merging the least influential factors. The refined results after pooling are shown in Tables 8 and 9. Table 8 reveals that productivity is mainly influenced by solar radiation, with a contribution of 50.45%, followed by water depth at 14.15% and water inlet temperature at 30.71%, with a minimal error of 4.69%. Table 9 shows that water temperature is predominantly influenced by solar radiation, accounting for 53.93% of the total variation, followed by wind velocity at 24.86% and water depth at 12.20%. The remaining 9.01% is attributed to experimental error. The regression equations (4) and (5) for productivity and water temperature were developed using the least squares method, which minimizes the sum of squared differences between observed and predicted values to obtain the best-fitting linear relationships between input parameters and responses. This statistical approach ensures that the coefficients accurately capture the impact of process variables on the system's performance.

$$\text{Productivity (kg/m}^2) = -0.869 + 0.000962 \text{ Solar radiation (W/m}^2) - 0.0549 \text{ Water Depth (cm)} + 0.0111 \text{ Wind velocity (m/s)} + 0.0306 \text{ Inlet Water temperature (˚C)} \quad \ldots (4)$$

$$\text{Water temperature (˚C)} = 42.45 + 0.00806 \text{ Solar radiation (W/m}^2) - 0.373 \text{ Water Depth (cm)} + 0.207 \text{ Wind velocity (m/s)} + 0.134 \text{ Inlet Water temperature (˚C)} \quad \ldots (5)$$

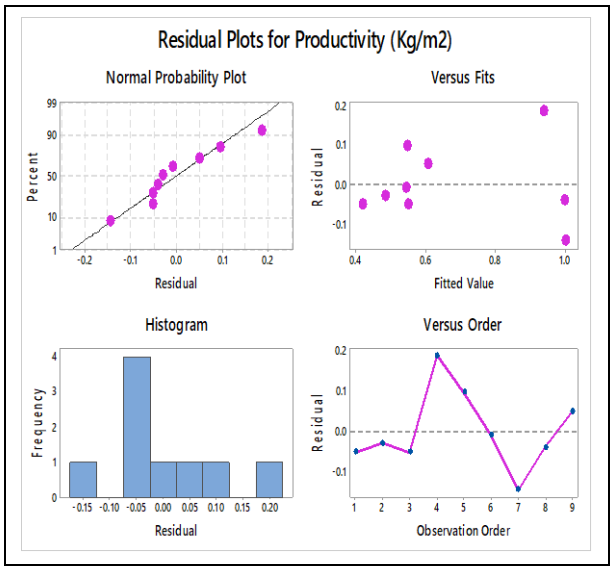


Fig. 6: Residual plots for Productivity

R^2 values of 95.31% for productivity and 90.99% for water temperature indicate a strong agreement between the predicted and experimental results, confirming the accuracy of the regression models (Li *et al.* 2024; Praveen *et al.* 2024).

Fig. 6 and Fig. 7 present the residual diagnostics for productivity and water temperature, respectively. The standard probability plots exhibit linear trends, confirming that the residuals are approximately normally distributed (Durakovic and Prakash, 2024). The residuals vs. fits plots show random dispersion around zero, confirming homoscedasticity. Histograms reveal approximately symmetric distributions without extreme outliers. The versus order plots exhibit no discernible trends or autocorrelation, validating the independence of residuals. Overall, the assumptions of linear regression are satisfied, affirming the statistical adequacy of the developed models (Kamalakannan *et al.* 2024; Shubham *et al.* 2025).

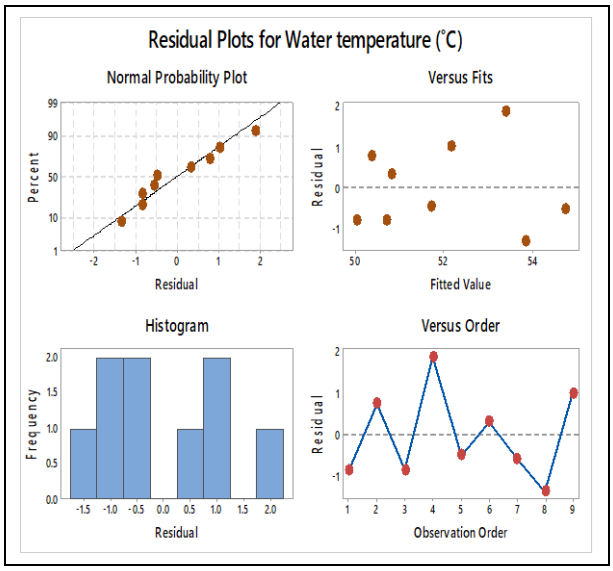


Fig. 7: Residual plots for Water temperature

Fig. 8 displays standard normal probability plots for both productivity and water temperature residuals, assessing the normality assumption of residuals essential for regression model validity. The mean productivity is 0.6758 kg/m² (SD: 0.2534), and the mean water temperature is 51.76 °C (SD: 1.660). The data points align well with the normal distribution and fall within the

95% confidence intervals, indicating a good fit. The Anderson-Darling (AD) statistics are 0.297 for productivity and 0.252 for water temperature, with corresponding p-values of 0.515 and 0.646, both of which are greater than the 0.05 significance level. This confirms that the datasets follow a normal distribution, validating the use of parametric statistical techniques in further analysis. Fig. 6 and Fig. 7 focus on residual patterns and spread, while Fig. 8 focuses on residual distribution normality (Chen *et al.* 2022; Kumar *et al.* 2022).

Table 10 presents the confirmation test results conducted at the optimal parameter settings identified through Taguchi analysis. The input parameters, including solar radiation (1000 W/m²), water depth (4 cm), inlet water temperature (40 °C), and wind velocity (3m/s), were selected based on their significant influence on system performance. Under these conditions, the predicted productivity was 1.131 kg/m², while the experimental value was 1.025 kg/m², resulting in a deviation of 9.31 %. For the basin water temperature, the predicted and the experimental values were 55 °C and 56.20 °C, respectively, with a deviation of only 2.18%. These results confirm the accuracy of the developed regression models and validate the effectiveness of the optimized parameter settings in enhancing the performance of the SS.

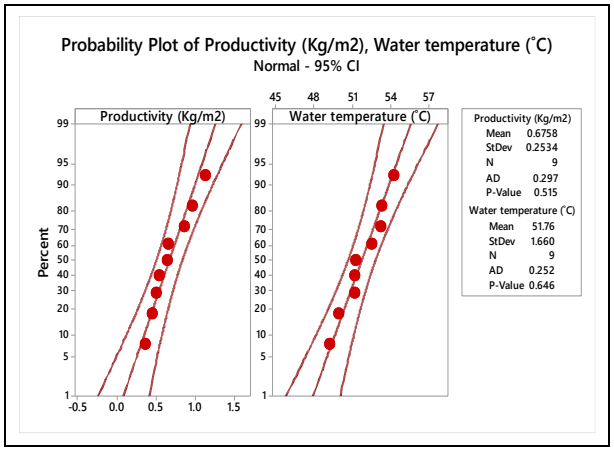


Fig. 8: Standard probability plots for Productivity and Water temperature

Table 10. Confirmation test results at optimal parameter settings

Optimal Level	Output Response	Predicted Value	Experimental Value	% Deviation
Solar radiation = 1000 W/m² Water depth = 4 cm Inlet water temperature = 40 ˚C Wind velocity = 3 m/s	Productivity (kg/m²)	1.131	1.025	9.31
	Basin Water Temperature (°C)	55	56.20	2.18

4. CONCLUSION

The study demonstrates that by optimizing the process parameters using the Taguchi method, the single slope solar still integrated with a solar pond achieved a maximum productivity of 1.131 kg/m² and a basin water temperature of 55 °C under optimal conditions of 1000 W/m² solar radiation, 4 cm water depth, 40 °C inlet water temperature, and 3 m/s wind velocity. The statistical analysis revealed that solar radiation contributed the most to productivity (50.45%), followed by inlet temperature (30.71%) and water depth (14.15%), while for water temperature, solar radiation accounted for 53.93%, wind velocity 24.86%, and water depth 12.20%, with low experimental errors of 4.69% and 9.01%, respectively. The regression models showed high predictive accuracy with R^2 values of 95.31% for productivity and 90.99% for water temperature, and the experimental validations indicated deviations of 9.31% in productivity and 2.18% in temperature, confirming model reliability and effective system performance enhancement.

Future research will concentrate on the application of advanced machine learning algorithms, including support vector machines and neural networks, to accurately predict the optimal operating conditions of SS. These models can capture complex nonlinear relationships and enhance performance prediction and system efficiency under varying environmental conditions.

FUNDING

This research received no specific grant from any funding agency in the public, commercial, or not-for-profit sectors.

CONFLICTS OF INTEREST

The authors declare that there is no conflict of interest.

COPYRIGHT

This article is an open-access article distributed under the terms and conditions of the Creative Commons Attribution (CC BY) license (http://creativecommons.org/licenses/by/4.0/)



REFERENCES

Abdulridha, H. O., Hameed, H. G.\, and Merzah, B. N., Performance study for single slope solar still integrated with different types of solar collectors, *Desalin. Water Treat.*, 319, 100538(2024). https://doi.org/10.1016/j.dwt.2024.100538

Aksoğan, K. A., and Toptaç, Y., Implementation of Taguchi method, ANOVA, and regression analyses to enhance char yield by carbonization in lignite-biomass blends. *Int. J. Coal Prep. Util.*, 45(2), 264–280(2025). https://doi.org/10.1080/19392699.2024.2333825

Almajali, T. A. H., Ismail, F. B., Gunnasegaran, P. A., Al Shurafa, S. M., and Kazem, H. A., Exploring the future of solar stills: recent breakthroughs in performance enhancement, *Sep. Purif. Rev.*, 54(2), 105–127(2025). https://doi.org/10.1080/15422119.2024.2366879

Antony, J., Bhat, S., Mittal, A., Jayaraman, R., Gijo, E. V., and Cudney, E. A., Application of Taguchi design of experiments in the food industry: a systematic literature review, *Tot. Qual. Manage. Bus. Excellence*, 35(5–6), 687–712(2024). https://doi.org/10.1080/14783363.2024.2331758

Ashok, R. and Sakthivel, T. G., A Complete Review of Augmenting Solar Desalination Efficiency with PCMs, *Res. Eng.*, 25, 104421(2025). https://doi.org/10.1016/j.rineng.2025.104421

Chen, W. H., Chen, K. H., Chein, R.Y., Ong, H. C. and Arunachalam, K. D., Optimization of hydrogen enrichment via palladium membrane in vacuum environments using Taguchi method and normalized regression analysis, *Int. J. Hydrogen Energy,* 47(100), 42280–42292 (2022). https://doi.org/10.1016/j.ijhydene.2022.01.060

Dhivagar, R. and Mohanraj, M., Optimization of performance of coarse aggregate-assisted single-slope solar still via Taguchi approach, *J. Renew. Energy Environ.*, 8(1), 13–19(2021). https://doi.org/10.30501/JREE.2020.232742.1112

Durakovic, B. and Prakash, M. K., Minimization of milling-induced residual stresses in AISI 1045 steel: process optimization using design of experiments taguchi method, *J. Mater. Eng. Perform.*, 33(15), 7721–7727(2024). https://doi.org/10.1007/s11665-024-09570-9

Fatima, F., Tiwari, N. P., and Singh, V., Process optimization for biosurfactant production by Bacillus aryabhattai SPS1001 using Taguchi method, *Appl. Biochem. Biotechnol.*, 197(1), 19–34(2025). https://doi.org/10.1007/s12010-024-05019-w

Hussein, A. K., Rashid, F. L., Rasul, M. K., Basem, A., Younis, O., Homod, R. Z., Attia, M. E. H. and Mudhar, A. A., Mohamed, B. B. H., Bagh, A. and Sajjad F. A., A review of the application of hybrid nanofluids in Solar still energy systems and guidelines for prospects, *Solar. Energy*, 272, 112485 (2024). https://doi.org/10.1016/j.solener.2024.112485

Jha, S. K. and Ghosh, A., Towards Sustainable Water Resources: A Critical Review of Evaluating Traditional and Solar-Based Desalination Technologies and Innovations, *Desalin. Water Treat.*, 322, 101246(2025). https://doi.org/10.1016/j.dwt.2025.101246

Kabeel, A. E., Attia, M. E. H., Abdelgaied, M., Essa, F. A. and Aboud, M. F. A., Comparative performance of spherical, hemispherical, and single-sloped solar distillers, *Desalin. Water Treat.*, 317, 100051(2024). https://doi.org/10.1016/j.dwt.2024.100051

Kamalakannan, V., Rajaram, S., Iyyadurai, J. and Arockiasamy, F. S., Fundamental study on influence of independent factors on response variable using response surface methodology and Taguchi method, *Eng. Proc.*, 61(1), 37(2024). https://doi.org/10.3390/engproc2024061037

Karthick, M., Joe, P. G. S., Appadurai, M. and Jeshurun, S. B., Productivity Enhancement of a Single Slope Solar Still with Energy Storage Medium, *Mater. Today: Proce.*, 60, 889–893(2022). https://doi.org/10.1016/j.matpr.2021.09.548

Kouravand, A., Shabestari, S. T., Zirak, N., Kasaeian, G., Fereidooni, L. and Kasaeian, A., Thermal management strategies for a portable double slope solar still with energy storage: An experimental study for enhancing the performance, *Next Energy,* 8, 100244(2025). https://doi.org/10.1016/j.nxener.2025.100244

Kumar, A., Rana, R. S., Purohit, R., Namdev, A., Saxena, K. K. and Atul, K., Optimization of dry sliding wear behavior of Si3N4 and Gr reinforced Al--Zn--Mg--Cu composites using taguchi method, *J. Mater. Res. Technol.*, 19, 4793–4803(2022). https://doi.org/10.1016/j.jmrt.2022.06.172

Kumar, V., Das, B. and Gupta, R., Energy, exergy, economic and environmental analyses of single slope solar still employing cylindrical cement fins and wick material for thermal energy storage, *J. Energy Storage*, 110, 115360(2025a). https://doi.org/10.1016/j.est.2025.115360

Kumar, V., Das, B. and Gupta, R., Performance enhancement of single slope solar still with sensible heat storage system: An experimental investigation under climatic conditions of Northeast India, *J. Sol. Energy Eng.*, 147(3), 031013 (2025).. https://doi.org/10.1115/1.4067663

Li, J., Huang, W., Xie, Y., Yang, J. and Zhao, M., The parameters optimization of robotic polishing with force controlled for mold steel based on Taguchi method, *J. Brazilian Soc. Mech. Sci. Eng*., 46(5), 313(2024). https://doi.org/10.1007/s40430-024-04889-9

Liu, H. and Zhu, W., Optimisation analysis by numerical simulation of adding internal fins in photovoltaic/thermal system based on Taguchi method, *Appl. Therm. Eng*., 266, 125635(2025). https://doi.org/10.1016/j.applthermaleng.2025.125635

Mohammed, A.H., Shmroukh, A.N., Ghazaly, N.M. and Kabeel, A.E., Performance analysis of an SPD integrated with a stepped pyramid solar still: Experimental study, *Environ. Dev. Sustain.*, 1–20 (2024). https://doi.org/10.1007/s10668-024-05272-3

Praveen, N., Mallik, U. S., Shivasiddaramaiah, A. G., Hosalli, R., Prasad, C. D. and Bavan, S., Machinability study of Cu-Al-Mn shape memory alloys using Taguchi method, *J. Inst. Eng. India Ser.*, 106(1), 231-243(2024). https://doi.org/10.1007/s40033-023-00629-w

Ramzy, K., Abdelgaleel, M., Kabeel, A. E. and Mosalam, H., Performance of a single slope solar still using different porous absorbing materials: an experimental approach, *Environ. Sci. Pollut. Res*., 30(28), 72398–72414(2023). https://doi.org/10.1007/s11356-023-27465-5

Saad, F. O., Mankai, S., Madiouli, J., Chemkhi, S., Shigidi, I. and Khan, M. I., Effect of phase change materials melting temperature on improving single slope solar still productivity, *J. Energy Storage,* 97, 112927(2024). https://doi.org/10.1016/j.est.2024.112927

Sahu, R. and Tiwari, A. C., Performance enhancement of single slope solar still using nanofluids at different water depth, *Desalin. Water Treat.*, 317, 100046 (2024). https://doi.org/10.1016/j.dwt.2024.100046

Shubham, S. K., Pandey, A. and Purohit, R., Study of tribological behavior using the Taguchi method and pin-on-disc machine along with mechanical properties of hybrid polymer composites, *Colloid Polym. Sci*., 303(4), 563-577(2025). https://doi.org/10.1007/s00396-025-05377-9

Thiyagarajan, P. K., Gokuldas, N. K., Rajendran, A. K., Saravanakumar, K. S., Vasudevan, M., Kannan, M., Prasad, C. D., Aden, A. A. and Srinivasa, G., Investigating the combinations of operating parameters of PEMFC computational results using the Taguchi Method, *Int. J. Thermofluids*, 27, 101162(2025). https://doi.org/10.1016/j.ijft.2025.101162

Yuvaperiyasamy, M., Senthilkumar, N. and Deepanraj, B., Experimental investigation on the performance of a pyramid solar still for varying water depth, contaminated water temperature, and addition of circular fins, *Int. J. Renew. Energy Develop*., 12(6), 1123–1130(2023). https://doi.org/10.14710/ijred.2023.57327

Yuvaperiyasamy, M., Senthilkumar, N. and Deepanraj, B., Enhancing Pyramid Solar Still Performance through Varied Heat Storage Materials and Water Depths: A Comprehensive Experimental Study, *Recent Patents Mech. Eng.*, 18(2), 148–157(2025). https://doi.org/10.2174/0122127976280612402280 45000